Materials Letters 156 (2015) 161–164

Contents lists available at ScienceDirect

Materials Letters

journal homepage: www.elsevier.com/locate/matlet

Three-fold improvement in the performance of all-polymer photovoltaic devices with graphene

Yan Jin, Fei Yu, Vikram K. Kuppa *

The Materials Science & Engineering Program, School of Biomedical, Chemical, and Environmental Engineering, University of Cincinnati, 501DERC, Cincinnati, OH 45221-0048, USA

ARTICLE INFO

Article history:
Received 30 December 2014
Accepted 21 April 2015
Available online 30 April 2015

Keywords:
Organic photovoltaics
Polymer blends
Polymer nanocomposites
Charge transport
Graphene
Efficiency

ABSTRACT

Solar cells fabricated from a blend of the conjugated polymers poly(3-hexylthiophene) (P3HT) and poly (9,9-dioctylfluorene-co-benzothiadiazole) (F8BT) demonstrate a substantial improvement in power conversion efficiency (η) upon the addition of pristine graphene to the active layer. Cells display complex dependence on graphene concentration, and a maximum of three-fold enhancement in performance. This increase is entirely due to the higher short circuit current (J_{sc}), since the open circuit voltage and fill factor are not affected. Cells also show greater bimolecular recombination with increasing graphene concentration. Device efficiency is demonstrated to be not only related to graphene content, but also to active layer thickness.

1. Introduction

Organic bulk heterojunction solar cells have attracted much attention due to their potential advantages of flexibility, low cost and ease of processing [1]. The classic bulk heterojunction involves a conjugated polymer mixed with fullerene derivatives [2], with efficiencies (η) exceeding 11% [3–6]. Another approach is the use of a blend of semiconducting polymers for exciton dissociation and charge transport [7,8], with the potential for enhanced spectral coverage. In general, blend devices are much less efficient, with a few exceptions [9,10]. This low performance is due to complex phase behavior [11,12], and because of considerably lower charge mobility [7]. One such typical blend system involves the semiconducting polymers poly(3-hexylthiophene) (P3HT) and poly (9,9-dioctylfluorene-co-benzothiadiazole) (F8BT). The absorption and fluorescence spectra of these polymers are complementary and they possess the requisite overlap of energy-levels for exciton dissociation at the interface. Nevertheless, blend performance is poor, with efficiencies of 0.13% when fabricated from *p*-xylene using a 60:40 weight ratio [13]. Efficiency was improved when processed using a solvent additive [14], by annealing [15], or by the addition of P3HT nanofibers [16].

Graphene is increasingly employed in optical devices and composite materials due to its excellent transmittance, high charge and thermal conductivity [17–19]. Pristine graphene possesses better electrical properties than both graphene oxide (GO) and reduced graphene oxide (RGO) [20,21]. Liu et al. fabricated BHJ devices based on P3HT and GO [22,23], achieving $\eta = 1.1\%$ for cells with 10% GO by weight, which is surprising because GO has low charge mobility [24]. Jun et al. [25] used RGO doped with nitrogen in P3HT/PCBM (1:1 weight ratio), and found a maximum of 40% increase in η. Yu et al. chemically grafted chains of P3HT onto RGO [26], and made bilayer cells with η of 0.6%. They also fullerene-doped RGO at 12 wt% in P3HT, to obtain BHJ cells with $\eta = 1.2\%$ [27]. Recently, a P3HT/PCBM (in a 1:1 weight ratio) cell showed a 15% increase in η with graphene, attributed to the increase in ambipolar mobility [28]. Our recent work has employed pristine graphene to improve the performance of P3HT/PCBM devices in an unconventional (10:1) weight ratio [29]. Our results demonstrated that it was possible to construct devices with a large fraction of the photoactive material, and yet retain the performance benefits of a traditional bulk heterojunction. In the present manuscript, we demonstrate results on a polymer blend of P3HT and F8BT, and show a three-fold increase in performance over unmodified systems with the addition of graphene.

2. Experimental details

P3HT ($M_w = 21{,}000$ g/mol, polydispersity = 1.6, regioregularity = 95%) and F8BT (Mn ~ 10,000–20,000 g/mol, PDI < 3) were obtained from Reike Metals and Sigma-Aldrich respectively. Pristine graphene (PG) was produced by solvent exfoliation of

* Corresponding author.
E-mail address: vikram.kuppa@uc.edu (V.K. Kuppa).

http://dx.doi.org/10.1016/j.matlet.2015.04.103
0167-577X/

graphite powder (300mesh, Alfa Aesar, 99.8% purity) in a C_6H_6/-C_6F_6 equimolar mixture [30]. The supernatant solution centrifuging (10,000 rpm, 1 min) has concentration of 0.2 mg/ml. PG was then transferred to *p*-xylene by evaporation of the C_6H_6/C_6F_6 at 100 C. Raman spectra showed a mixture of mono- and multi-layer flakes. The lateral size was 200 nm, using dynamic light scattering [31]. Cells were fabricated in N_2 by spin-coating P3HT/F8BT/PG from *p*-xylene onto PEDOT:PSS (50 nm) coated ITO/glass substrates. P3HT and F8BT were always present in a 6:4 weight ratio, but the concentration varied between 6 and 10 mg/mol to vary device thickness. Cells were soft-baked for 30 minutes in N_2 at 50 C, followed by thermal evaporation of LiF (~1 nm) and Al (200 nm). Final annealing was at 150 C for 10 min in N_2. The current–voltage characteristics of devices were measured by an electrometer (Keithley) under AM1.5 G illumination (irradiation intensity is 100 mW/cm^2) with effective device area of 2×2 mm^2 provided by using a shadow mask. External quantum efficiency (EQE) measurements were conducted using a dual-channel Merlin lock-in amplifier, optical chopper and Si-detector, using the same Xe lamp as that used in the JV white light measurements. The polymer film thicknesses were measured by a surface profiler (TENCOR P-10). The power conversion efficiency (η) was calculated by maximum output power divided by the illumination intensity.

3. Results and discussion

Fig. 1 shows the efficiency (η) and short-circuit current density (J_{sc}) of cells made from P3HT/F8BT (6/4 mg/ml) as a function of graphene concentration. Both η and J_{sc} increase sharply, reaching a maximum at 0.1 mg/ml; J_{sc} rises from 0.2 mA/cm^2 to 0.52 mA/cm^2, while η is improved from 0.052% to a maximum of 0.14%, a nearly threefold enhancement in performance over cells without PG. Fig. 1 in supplementary information shows the *J*–*V* curves of cells in dark and under illumination. Detailed cell parameters including the open circuit voltage (V_{oc}) and the fill-factor (FF), are shown in Table 1 (Tables 1 and 2 in supplementary information list the series resistance with different thickness/roughness for every PG concentration). Neither V_{oc} nor FF are significantly affected by graphene. The high efficiency is therefore entirely derived from the greater current engendered by PG addition, which enhances both charge collection and transport [18,25]. J_{sc} initially increases because PG enables pathways for charge transport. However, this increase is not monotonic, for two reasons; first, since PG is a an excellent conductor of both electrons and holes, it can act as a recombination center; second, beyond a certain limit, PG is not well dispersed in the polymer matrix, but rather agglomerates and falls out of solution, leading to short-circuiting of the cell. Our results are consistent with the percolation of PG across the active layer between the ITO and Al electrodes. A qualitatively similar dependence on concentration has been seen earlier in P3HT/PCBM solar cells doped with carbon nanotubes [32].

Fig. 2 shows the external quantum efficiency (EQE) of cells under AM1.5 radiation. The EQE is enhanced with the addition of graphene, and is the highest for PG concentrations of 0.1 mg/ml. The varying EQEs reveal changes in polymer morphology with the introduction of graphene. The increase in EQE is manifested over a broad spectrum (300–650 nm) but is prominent in the 450–650 nm range. The increase in this region has a much greater relative increase [~200% vs 50%] than over the shorter wavelengths, indicating a greater contribution due to P3HT chain reorganization in the presence of PG [12]. Specifically, the structural features are identified planar chains that form weakly interacting H-aggregates [33,34]. Other groups [12] have noted that the interaction of F8BT with P3HT in solid-state blends appears to hinder ordering of P3HT. However, the addition of graphene to the blend advances phase separation and

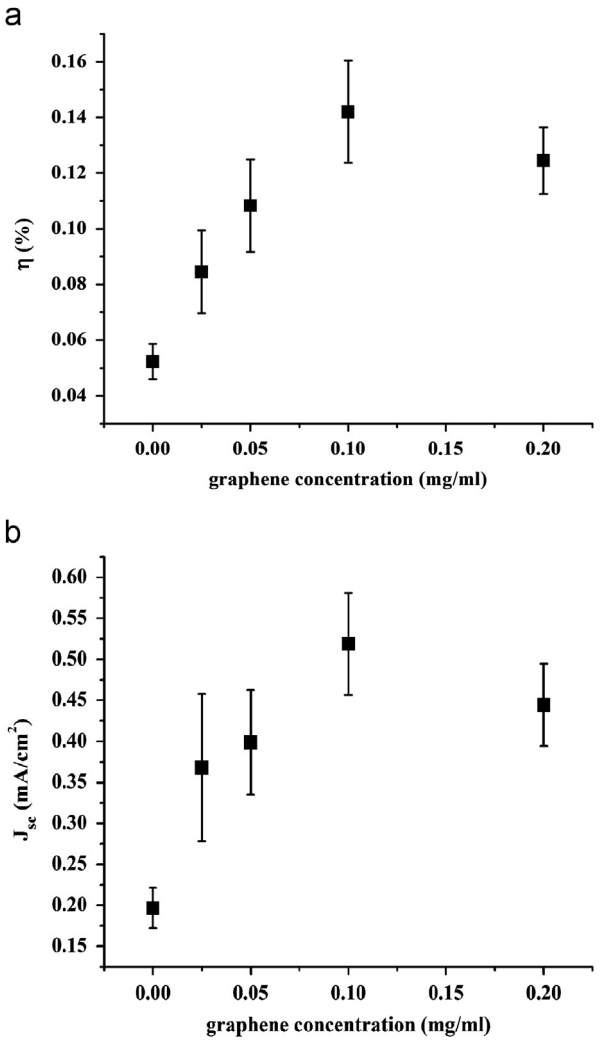

Fig. 1. (a) η and (b) J_{sc} of P3HT/F8BT cells as a function of graphene concentration.

Table 1
Parameters and efficiencies of photovoltaic devices with P3HT/F8BT (6/4 weight ratio, 10 mg/ml in *p*-xylene) at different graphene concentrations.

	V_{oc} (V)	J_{sc} (mA/cm^2)	FF (%)	η (%)	Thickness (nm)
P3HT/F8BT	1.37	0.20	19	0.052	63.5 ± 9.1
P3HT/F8BT/0.025 G	1.14	0.37	21	0.085	66.7 ± 5.7
P3HT/F8BT/0.05 G	1.39	0.40	20	0.108	73.7 ± 5.7
P3HT/F8BT/0.1 G	1.35	0.52	20	0.142	85 ± 4.6
P3HT/F8BT/0.2 G	1.30	0.44	22	0.125	91.3 ± 7.6

aggregate formation [35], since P3HT adsorbs more readily on the sp^2 conjugated hexagonal structure of graphene.

J_{sc} values were also recorded under different illumination intensities to probe charge transport and recombination behavior [36,37]. At low intensity, monomolecular recombination occurs, in which one mobile charge recombines with an immobile trapped charge, while bimolecular recombination occurs when two mobile charges neutralize each other after diffusion [38,39]. As the light intensity increases, charge carrier density increases, and bimolecular recombination is much more likely [38,40] A scaling relation between the J_{sc} and intensity is:

$$J_{sc} \sim I^{\alpha} \quad ; \quad \log J_{sc} \sim \alpha \cdot \mathrm{Log}\ I \tag{1}$$

The exponent α in the equation (1) reveals the recombination mechanism. α close to 1 indicates monomolecular kinetics, while